Comparison of 1-^{11}C-Glucose and ^{18}F-FDG for Quantifying Myocardial Glucose Use with PET

Pilar Herrero, MS[1]; Terry L. Sharp[1]; Carmen Dence, MS[1]; Brendan M. Haraden, MD[2]; and Robert J. Gropler, MD[1,2]

[1]Cardiovascular Imaging Laboratory, Division of Radiological Sciences, Mallinckrodt Institute of Radiology, Washington University School of Medicine, St. Louis, Missouri; and [2]Cardiovascular Division, Department of Internal Medicine, Washington University School of Medicine, St. Louis, Missouri

In this study, we compared the accuracy of the rate of myocardial glucose use (rMGU) measured using PET and 1-^{11}C-glucose with the rate measured using PET and the more conventional tracer ^{18}F-FDG. **Methods:** PET measurements of myocardial tracer uptake (K, in mL/g/min) and rMGU (in nmol/g/min) were obtained with 1-^{11}C-glucose and ^{18}F-FDG in 21 dogs using kinetic modeling and the Patlak graphical method, respectively. Eighteen dogs were studied during hyperinsulinemic–euglycemic clamp performed either at rest or combined with phenylephrine, dobutamine, intralipid infusion, or intralipid infusion and dobutamine. Three dogs were studied during intralipid infusion alone under resting conditions. Arterial–coronary sinus sampling was performed to measure the K of both tracers ($n = 14$) and rMGU by the Fick method ($n = 21$). **Results:** PET-derived values for K from either 1-^{11}C-glucose or ^{18}F-FDG correlated closely with directly measured tracer K values (glucose: $y = 0.98x + 0.01$, $r = 0.79$, $P < 0.001$; ^{18}F-FDG: $y = 0.74x + 0.03$, $r = 0.77$, $P < 0.001$). In contrast, correlation with K values of unlabeled glucose measured directly was better for 1-^{11}C-glucose ($y = 0.92x + 0.02$, $r = 0.96$, $P < 0.0001$) than for ^{18}F-FDG ($y = 0.66x + 0.05$, $r = 0.72$, $P < 0.01$) ($P < 0.001$ for comparison of correlation coefficients). As a consequence, PET-derived values for rMGU correlated more closely with Fick-derived measurements of unlabeled glucose using 1-^{11}C-glucose ($y = 0.82x + 168$, $r = 0.97$, $P < 0.0001$) than with ^{18}F-FDG ($y = 0.81x + 278$, $r = 0.79$, $P < 0.001$) ($P < 0.001$ for comparison of correlation coefficients). **Conclusion:** Over a wide range of conditions, PET-derived measurements of rMGU are obtained more accurately with 1-^{11}C-glucose than with ^{18}F-FDG.

Key Words: glucose; metabolism; myocardium; tomography

J Nucl Med 2002; 43:1530–1541

Quantification of the rate of myocardial glucose use (rMGU) plays a key role in furthering our understanding of normal cardiac development and physiology and of a variety of cardiac disease processes such as myocardial ischemia, left ventricular hypertrophy, and cardiomyopathy (*1–4*). To date, PET using ^{18}F-FDG has been the most common method to noninvasively quantify rMGU. Recently, our group reported that rMGU could be quantified by PET using glucose radiolabeled in the 1-carbon position with ^{11}C (1-^{11}C-glucose) (*5*).

Both tracers offer significant advantages and disadvantages for quantifying rMGU with PET. For example, the myocardial kinetics of ^{18}F-FDG have been well characterized, and this tracer has been used to quantify rMGU with PET for nearly 20 y (*6–10*). The acquisition scheme is relatively straightforward. The synthesis procedures for producing ^{18}F-FDG have been automated and produce large amounts of radiopharmaceutical. When coupled with the relatively long physical half-life of ^{18}F (approximately 110 min), this advantage permits offsite production of ^{18}F-FDG with delivery to multiple imaging centers. The demonstrated efficacy of ^{18}F-FDG uptake to differentiate malignant (high uptake) from benign (low uptake) tumors has led to the rapid growth of clinical PET. That being said, quantifying rMGU with PET and ^{18}F-FDG suffers from several disadvantages. The most prominent is that because ^{18}F-FDG is a glucose analog, its initial uptake and phosphorylation differ from those of glucose. Consequently, a correction factor that accounts for these differences, called the lumped constant (LC), must be known to accurately quantify rMGU with ^{18}F-FDG. However, it is well established that the LC can vary with the availability of insulin and fatty acids in plasma and with the level of blood flow (*11–15*). Although an approach has been devised to correct for the variability in the level of plasma fatty acids and insulin, the accuracy of the method has been validated only in isolated perfused hearts, not in vivo (*16*). Other disadvantages of ^{18}F-FDG include the limited metabolic fate of ^{18}F-FDG in tissue, precluding determination of the metabolic fate (i.e., glycogen formation vs. glycolysis) of the extracted tracer and glucose, and limitations on the performance of serial measurements of rMGU because of the relatively long physical half-life of ^{18}F (approximately 110 min).

PET with 1-^{11}C-glucose also offers several advantages over PET with ^{18}F-FDG for quantifying rMGU. Because

Received Oct. 22, 2001; revision accepted Mar. 25, 2002.

For correspondence or reprints contact: Pilar Herrero, MS, Cardiovascular Imaging Laboratory, Mallinckrodt Institute of Radiology, 510 S. Kingshighway Blvd., St. Louis, MO 63110.

E-mail: HerreroP@mir.wustl.edu

glucose has been labeled with ^{11}C, its metabolic fate in myocardium is identical to that of glucose. Consequently, no corrections are necessary to account for differences in the myocardial kinetics of 1-^{11}C-glucose relative to unlabeled glucose. An appropriate compartmental model has been developed to characterize the kinetics of this tracer and permits accurate measurements of rMGU (*5*). Another advantage of 1-^{11}C-glucose is the short physical half-life of ^{11}C (approximately 20 min), making serial measurements of rMGU possible. However, there are several disadvantages to using this tracer. Most notable is the limited experience in measuring rMGU with 1-^{11}C-glucose, with only 1 study reported in the literature (*5*). The acquisition scheme to quantify rMGU using 1-^{11}C-glucose is more complex than that using ^{18}F-FDG because of the need to correct the arterial input function for the production of $^{11}CO_2$ and ^{11}C-lactate. Unlike the procedure for ^{18}F-FDG, the current synthesis procedure for 1-^{11}C-glucose is not as routine and produces much less radiopharmaceutical. The short physical half-life of ^{11}C, coupled with the low production yield, requires an on-site cyclotron for PET studies using this tracer. Finally, except for measurements of the rate of cerebral glucose use (*17*,*18*), 1-^{11}C-glucose has not yet been shown to be useful for other noncardiac applications, such as oncologic applications.

Because of the advantages and disadvantages of the 2 methods to measure rMGU, understanding the relative accuracy of PET using either ^{18}F-FDG or 1-^{11}C-glucose to quantify rMGU is important. Accordingly, the goal of this study was to determine the accuracy of measurements of rMGU using these 2 methods in a well-controlled canine model over a wide range of rMGU and plasma insulin and fatty acid availability.

MATERIALS AND METHODS

Animal Preparation

All animal experiments were conducted in compliance with the Guidelines for the Care and Use of Research Animals established by the Animal Studies Committee at Washington University. The animals fasted for 12–18 h before they received subcutaneous premedication with 1–2 mg/kg of morphine sulfate. Thirty to 60 min after the premedication, the animals were anesthetized with sodium thiopental (12.5 mg/kg) and were then given intravenous α-chloralose (72 mg/kg). The animals were intubated and ventilated with room air and supplemental oxygen to maintain arterial blood gases within the physiologic range. After the induction of anesthesia and intubation, catheters were placed in the thoracic aorta through the femoral arteries for monitoring arterial blood pressure and for arterial sampling. One femoral vein was cannulated to obtain venous samples and to administer drugs. The right external jugular vein was exposed for placement of a coronary sinus catheter. The coronary sinus catheter was placed under fluoroscopic guidance, and its location was verified by contrast injection and measurement of the oxygen saturation of coronary sinus blood.

To define the myocardial kinetics of 1-^{11}C-glucose and ^{18}F-FDG over a wide range of substrate, hormonal, and cardiac work conditions, we performed the following interventions on 21 dogs. Three dogs were studied at rest during the intravenous infusion of 20% Intralipid (Pharmacia Inc., Clayton, NC) at a rate of 1 mL/min. This intervention was designed to significantly raise plasma fatty acid levels and, thus, lower rMGU. The results from these 3 dog studies were reported previously (*5*). The other 18 dogs were studied during a hyperinsulinemic–euglycemic clamp (HIC) as described previously (*5*). Nine dogs were studied during the clamp at rest, a condition that would be expected to increase rMGU. To further increase rMGU, 3 dogs were studied during the coadministration of phenylephrine (0.84–1.6 μg/kg/min), a predominantly α-adrenergic agonist. These dogs were supplemented with intermittent boluses of intravenous atropine (0.5 mg) to maintain the heart rate at preinfusion rates. Two dogs were studied during coadministration of the clamp and dobutamine (10 μg/kg/min), a predominantly β-adrenergic agonist. It was anticipated that the peripheral lipolytic effects of β-adrenergic stimulation would markedly increase plasma fatty acids levels and decrease rMGU. To determine further how well each tracer performed when both plasma insulin and fatty acids were increased, 2 dogs were studied during coadministration of the clamp and lipid infusion. To assess the additive effects of increased cardiac work, 2 dogs were studied during the clamp, lipid infusion, and dobutamine. After completion of the PET study, the animals were euthanized with an overdose of anesthesia and KCl.

Imaging Protocol

1-^{11}C-glucose was synthesized according to a published procedure (*19*,*20*). All PET studies were performed on an ECAT-EXACT 962 HR+ scanner (Siemens, Knoxville, TN). The electrocardiogram, hemodynamics, and blood gas values were monitored throughout the study. A transmission scan was obtained to correct for photon attenuation. To measure myocardial perfusion, 14.8 MBq/kg of ^{15}O-water were administered as an intravenous bolus, and dynamic PET data were acquired for 5 min. After allowing for decay of ^{15}O radioactivity, 555–740 MBq of 1-^{11}C-glucose were administered as a bolus, followed by 60 min of dynamic data collection. After allowing for decay of the ^{11}C-activity, the ^{15}O-water scan was repeated. Then, 296–370 MBq of ^{18}F-FDG were administered as a bolus, followed by 60 min of dynamic data collection. Plasma ^{11}C activity and ^{18}F-FDG activity were measured in paired arterial and coronary sinus blood samples that were obtained during the imaging sessions for 14 dogs. This procedure permitted direct measurements of myocardial extraction of both 1-^{11}C-glucose and ^{18}F-FDG. To measure rMGU and myocardial oxygen consumption (MVO_2) on the basis of the myocardial extraction of glucose and oxygen, respectively, arterial and coronary sinus blood samples for glucose and oxygen were obtained at the beginning, middle, and end of the scanning intervals for all 21 dogs. To verify the stability of the substrate environment, fatty acids, lactate, and insulin were obtained at the same intervals. In addition, arterial and coronary sinus plasma samples were obtained during 1-^{11}C-glucose imaging for all 21 dogs to measure the production of $^{11}CO_2$ and ^{11}C-lactate. Arterial levels of these labeled glucose metabolites were used to obtain a correct arterial input function for modeling of the myocardial kinetics of 1-^{11}C-glucose.

Analysis of PET Data

Myocardial ^{15}O-water, 1-^{11}C-glucose, and ^{18}F-FDG images were reoriented to generate standard short-axis and long-axis views. Composite PET images of myocardial ^{11}C or ^{18}F activity

representing 30–60 min after injection were generated for placement of regions of interest (*5*). To generate myocardial time–activity curves, regions of interest encompassing the anterolateral–anteroinferior wall (5–7 cm^3) were placed on 3–5 midventricular short-axis slices of the composite image. To obtain the input function, a small region of interest (1 cm^3) was placed within the left atrial cavity on a midventricular slice in the vertical long-axis orientation. Within these regions of interest, myocardial and blood time–activity curves were generated for ^{15}O-water, 1-^{11}C-glucose, and ^{18}F-FDG. To avoid contamination from right ventricular blood radioactivity, septal regions were omitted. Subsequently, values for myocardial blood flow (MBF, mL/g/min), myocardial glucose uptake for 1-^{11}C-glucose and ^{18}F-FDG (K, mL/g/min), and glucose use from either 1-^{11}C-glucose or ^{18}F-FDG K values (rMGU, nmol/g/min) were calculated for each region of interest and averaged to obtain 1 mean value for MBF (from ^{15}O-water) and K and rMGU (for 1-^{11}C-glucose and ^{18}F-FDG) per dog. These values were then compared with global measurements of left ventricular uptake of tracer or unlabeled glucose performed using the Fick method. To compare the regional variability of PET-derived 1-^{11}C-glucose and ^{18}F-FDG K values, the regional coefficient of variation (COV%) for K was calculated as the ratio of the regional SD to the mean, multiplied by 100.

Measurement of MBF. Applying the image-analysis routine to the time-segmented data allowed generation of blood and myocardial time–activity curves for each segment. From these data, MBF was quantified using a compartmental modeling approach developed and validated previously at this institution (*21–23*).

Measurement of rMGU Using 1-^{11}C-Glucose. PET blood (corrected for $^{11}CO_2$ and ^{11}C-lactate) and myocardial time–activity curve data were analyzed using a 4-compartment model developed and validated previously in our laboratory (*5*). In brief, vascular 1-^{11}C-glucose enters the interstitial and cytosolic component of the myocardium (compartment 1) at a rate of K_1 (mL/g/min). Once the tracer is in compartment 1, either it diffuses back into the vasculature at a rate of k_2 (min^{-1}) or it is phosphorylated and metabolized to pyruvate (compartment 2) at a rate of k_3 (min^{-1}). Label can either form glycogen (compartment 3) at a rate of k_4 (min^{-1}) or be metabolized through anaerobic or oxidative pathways (compartment 4) at rate of k_5 (min^{-1}). Tracer entering the metabolic compartment is assumed to be unidirectional, and washout of $^{11}CO_2$ and ^{11}C-lactate to the vasculature is assumed to be proportional to flow. Myocardial time–activity curves were corrected for partial-volume effects a priori using the fractional tissue recovery coefficient obtained from the ^{15}O-water model. The model transfer rate-constants (K_1, k_2–k_5) and the spillover fraction (*22*) were estimated using well-established numeric methods (*24,25*). Steady-state conditions were assumed, and K and rMGU were then calculated from these rates as follows:

$$K\ (mL/g/min) = (K_1 \times k_3)/(k_2 + k_3)\ \text{and} \qquad \text{Eq. 1}$$

$$rMGU\ (nmol/g/min) = Gl_b \times K, \qquad \text{Eq. 2}$$

where Gl_b is plasma glucose level, in nmol/mL.

Measurement of rMGU Using ^{18}F-FDG. Measurements of rMGU using ^{18}F-FDG kinetic data were done by 2 different methods, the Patlak method and compartmental modeling. Because it is the most commonly used method to quantify rMGU by PET and ^{18}F-FDG, the Patlak method was chosen to compare rMGU measurements obtained from 1-^{11}C-glucose with those derived from ^{18}F-FDG. However, because ^{18}F-FDG kinetics are described more accurately by compartmental modeling than by the Patlak method when ^{18}F-FDG egress or dephosphorylation is present, compartmental modeling was also implemented to compare rMGU measurements obtained from the Patlak method with those obtained from ^{18}F-FDG kinetic modeling.

Myocardial glucose uptake was estimated from PET-derived blood and myocardial ^{18}F-FDG time–activity curves using Patlak graphic analysis (*8*). This method, which can be applied to kinetic models in which the tracer is assumed to be irreversibly trapped, can be used to calculate net tracer uptake, with K as the slope of the linear equation:

$$Cm(t)/Cb(t) = K \times \left[\int_0^t Cb(t)\ ds\right]/Cb(t) + W, \qquad \text{Eq. 3}$$

where Cm(t) (cpm/g/mL) is myocardial activity at time t, Cb(t) (cpm/g/mL) is blood activity at time t, K is net tracer uptake (mL/g/min), $\int_0^t Cb(t)\ ds$ (cpm × min) is the integral of plasma activity from time zero to time t, and W is a parameter depending on the steady-state volume of the reversible compartments and the effective plasma volume.

Myocardial time–activity curves were corrected for partial-volume effects a priori using the fractional tissue recovery coefficient obtained from the ^{15}O-water model. To estimate K from Equation 3, PET blood and myocardial ^{18}F-FDG time–activity curves were used to generate 6 sets of *x–y* data points representing data at 2, 5, 9, 18, 36, and 56 min after injection of tracer. To show the linearity of the dataset, data points were plotted on an *x–y* plot and points that visually diverged from a straight line were excluded from the analysis. On average, the last 2 sets of data points, representing data collected at 36 and 56 min after ^{18}F-FDG injection, were excluded from the analysis. No early points were excluded. To account for the differences in uptake and phosphorylation of ^{18}F-FDG and glucose, K values obtained from Equation 2 were corrected by an LC value of 0.67 (*6*). Furthermore, because more recent studies have shown that the value of the LC varies with varying substrate, hormonal, and work environment (*11–15*), K values were also corrected by a variable LC, as defined by Wiggers et al. (*26*), as follows:

$$LCv = Rp + (Rt - Rp) \times K/K_1, \qquad \text{Eq. 4}$$

where Rp is a known ratio between the rates of phosphorylation of ^{18}F-FDG and glucose (0.43), Rt is a known ratio between the rates of membrane transport of ^{18}F-FDG and glucose (2.26), K (mL/g/min) is net ^{18}F-FDG uptake (estimated from Patlak analysis), and K_1 is unidirectional ^{18}F-FDG transport (mL/g/min) (estimated from kinetic modeling of ^{18}F-FDG kinetics). Using Equation 2, rMGU was calculated from uncorrected and corrected K values.

A previously validated 3-compartment kinetic model, originally developed for calculation of the rate of cerebral glucose use and subsequently modified for the heart, was used (*7*). The individual rate constants describing the forward (K_1, mL/g/min) and reverse (k_2, min^{-1}) transport of ^{18}F-FDG across the sarcolemma, the hexokinase-mediated phosphorylation of ^{18}F-FDG (k_3, min^{-1}) and dephosphorylation of ^{18}F-FDG (k_4, min^{-1}), and the spillover fraction (as a fifth parameter) were estimated by fitting the model to the myocardial tissue time–activity curves using a nonlinear least-squares algorithm. All of the myocardial time–activity curves were precorrected for the partial-volume effect using correction factors

calculated for the measurement of MBF with ^{15}O-water. Then, for each region of interest, ^{18}F-FDG tracer uptake (K, mL/g/min) was calculated from the estimated rate constants twice, assuming that ^{18}F-FDG egress or dephosphorylation was negligible (i.e., $k_4 = 0$) and that ^{18}F-FDG egress or dephosphorylation was not negligible (i.e., $k_4 \neq 0$).

Measurement of Radioactive Plasma Metabolites and Myocardial Tracer Uptake

Total ^{11}C-activity and ^{18}F-FDG activity in arterial and coronary sinus plasma were measured in a well counter (model 1000; Canberra, Meridien, CT). Total 1-^{11}C-glucose activity was calculated from ^{11}C-activity as follows: Total ^{11}C-acidic metabolites (^{11}C-lactate and $^{11}CO_2$) were first separated from neutral sugars by trapping them in an ion exchange column (AG1-X4 resin, 100–200 mesh, formate form). The plasma sample was then eluted through this column with 5 mL of water. Both resin and eluate were counted for radioactivity to obtain the total acidic metabolites and nonmetabolized glucose present (1-^{11}C-glucose). To measure ^{11}C-lactate and $^{11}CO_2$ from total acidic metabolites, a similar serum sample was also deposited in a test tube, acidified with 6N HCl, sparred with N_2 for 10 min to eliminate the $^{11}CO_2$, and counted for radioactivity against a sample kept under basic conditions. The count difference between the test tubes was used to calculate the percentage of $^{11}CO_2$ in the plasma sample. To obtain the percentage of ^{11}C-lactate, the percentage of $^{11}CO_2$ was subtracted from the total percentage of acidic metabolites in the resin. The myocardial extraction fractions for 1-^{11}C-glucose and ^{18}F-FDG were calculated as the difference between the arterial and coronary sinus plasma values divided by the arterial plasma values for 1-^{11}C-glucose and ^{18}F-FDG activity, respectively. Myocardial uptake of the tracers (K, mL/g/min) was then calculated as the product of the extraction fraction (unitless) and MBF (mL/g/min).

Measurement of Myocardial Uptake and Use of Unlabeled Glucose

The extraction fraction for unlabeled glucose was calculated from each of the 3 sets of blood samples taken during the glucose study as the ratio of the difference between plasma levels of arterial and coronary sinus glucose divided by the arterial glucose level. Glucose uptake (K, mL/g/min) was then calculated as the product of glucose extraction fraction (unitless) and MBF (mL/g/min), and glucose use (nmol/g/min) was calculated as the product of glucose uptake and the arterial plasma glucose level (nmol/mL). A mean value per study was obtained by averaging values obtained from the 3 sets of blood samples.

Measurement of Plasma Insulin and Unlabeled Substrates

Plasma insulin levels were measured by radioimmunoassay (*27*). Glucose and lactate were assayed enzymatically using a commercially available glucose-lactate analyzer (YSI, Yellow Springs, OH). Fatty acids in plasma were determined by capillary gas chromatography and high-performance liquid chromatography (*5*).

Statistical Analysis

All data are presented as the mean ± SD. Correlations were calculated by linear regression. Differences in slopes were compared using a 2-tailed *t* test. Correlation coefficients were compared using a Fisher *z* transformation and a 2-tailed Z test. Because of the small sample size of most groups studied, no statistical analyses were performed on the group means presented in Tables 1–4.

RESULTS

Hemodynamics, Myocardial Perfusion, and MVO_2

Measurements of hemodynamics, MBF, and MVO_2 for the 6 groups of dogs during both the 1-^{11}C-glucose and the ^{18}F-FDG scans are shown in Tables 1 and 2. As expected, an increase in the rate–pressure product (RPP) was observed in the dogs receiving phenylephrine with atropine supplementation, reflecting elevations in both systolic blood pressure and heart rate. Primarily because of an increase in heart rate, the RPP was increased in dogs undergoing both the HIC and dobutamine administration. The heart rate and systolic blood pressure were increased in the groups receiving Intralipid either alone at rest or during the coadministration of dobutamine, consistent with the increase in α_1-receptor sensitivity associated with infusion of lipid emulsions (*28*). This resulted in an increased RPP. In dogs receiving intralipid and the insulin clamp, the RPP did not increase, primarily because the heart rate did not increase. The etiology of the lack of increase in heart rate is unclear. In general, the increased levels in RPP were paralleled by increases in both MBF and MVO_2. Values for MBF and

TABLE 1
Hemodynamics, MBF, and MVO_2 During 1-^{11}C-Glucose Study

Intervention	Blood pressure (mm Hg)		Heart rate (bpm)	RPP (mm Hg × bpm)	MBF (mL/g/min)	MVO_2 (μmol/g/min)
	Systolic	Diastolic				
HIC/R (*n* = 9)	120 ± 18	79 ± 14	88 ± 19	8,157 ± 2,154	0.89 ± 0.15	9.05 ± 2.14
HIC/D (*n* = 2)	115 ± 31	66 ± 5	200 ± 1	16,602 ± 2,736	2.15 ± 0.07	32.5 ± 7.14
HIC/PHEN (*n* = 3)	199 ± 63	132 ± 51	123 ± 23	18,915 ± 7,366	1.53 ± 0.46	26.58 ± 6.30
IL/R (*n* = 3)	173 ± 13	122 ± 14	114 ± 70	15,882 ± 10	0.91 ± 0.32	15.7 ± 4.61
IL/HIC (*n* = 2)	180 ± 4	114 ± 11	75 ± 16	10,362 ± 2,858	0.67 ± 0.21	15.3 ± 0.70
IL/HIC/D (*n* = 2)	160 ± 25	101 ± 6	142 ± 9	17,138 ± 637	2.27 ± 0.57	41.96 ± 11.03

D = dobutamine.
Values represent mean ± SD.

TABLE 2
Hemodynamics, MBF, and MVO_2 During ^{18}F-FDG Study

Intervention	Blood pressure (mm Hg)		Heart rate (bpm)	RPP (mm Hg × bpm)	MBF (mL/g/min)	MVO_2 (μmol/g/min)
	Systolic	Diastolic				
HIC/R (n = 9)	120 ± 24	81 ± 15	96 ± 37	9,165 ± 4,488	0.85 ± 0.21	8.40 ± 2.45
HIC/D (n = 2)	129 ± 39	75 ± 11	182 ± 7	17,139 ± 4,314	2.62 ± 0.59	34.64 ± 18.90
HIC/PHEN (n = 3)	153 ± 25	104 ± 10	120 ± 19	14,290 ± 1,872	1.66 ± 0.22	24.36 ± 10.40
IL/R (n = 3)	147 ± 41	103 ± 36	161 ± 98	16,554 ± 5,067	0.82 ± 0.38	14.23 ± 6.52
IL/HIC (n = 2)	177 ± 11	116 ± 19	82 ± 11	11,312 ± 2,881	0.65 ± 0.00	11.61 ± 0.13
IL/HIC/D (n = 2)	172 ± 32	103 ± 19	140 ± 53	17,154 ± 3,430	2.09 ± 0.79	36.43 ± 15.09

D = dobutamine.
Values represent mean ± SD.

MVO_2 tended to be higher in the dogs receiving dobutamine than in the dogs receiving phenylephrine, a finding that may well reflect the combined effects of vasodilation due to β_2-adrenergic stimulation and the increased oxygen demands of fatty acid metabolism. Also of note, there was a trend toward a lower level of MBF despite an increase in the RPP in the dogs receiving intralipids under resting conditions. This blunting of MBF may reflect the inhibitory effects of high plasma fatty acids on endothelial function (*29*). Finally, it should be noted that similar hemodynamic, MBF, and MVO_2 responses to each intervention were observed during the 1-^{11}C-glucose and ^{18}F-FDG imaging studies.

Plasma Substrate Levels and Myocardial Substrate Use

Shown in Tables 3 and 4 are the arterial plasma levels for glucose, free fatty acids, lactate, and insulin levels, as well as rMGU values measured during the 1-^{11}C-glucose and ^{18}F-FDG scans for all interventions. Plasma glucose and lactate levels were similar between the groups. Plasma fatty acid levels were higher in all groups receiving a lipid infusion. The fatty acid levels were the lowest in the dogs undergoing the insulin clamp at rest, consistent with the lipid-storing effects of this hormone. As designed, plasma insulin levels were increased in all groups undergoing the insulin clamp. The insulin levels were lowest in dogs studied at rest during the infusion of lipids. These changes in substrate and insulin plasma levels, as well as the changes in myocardial work induced by the different physiologic interventions performed, resulted in a wide range of rMGU levels. Dogs studied during intralipid infusion at rest had the lowest rMGU levels. Increases in rMGU were observed during HIC and were offset by the concomitant infusion of intralipid. As expected, the highest levels of rMGU were observed in dogs undergoing the insulin clamp and receiving phenylephrine. Levels of plasma substrates, insulin, and rMGU during the different interventions were similar during the 1-^{11}C-glucose and ^{18}F-FDG imaging studies.

PET Data Analysis

Representative myocardial images of 1-^{11}C-glucose and ^{18}F-FDG are shown in Figure 1. As expected, differential myocardial uptake of both tracers increased with increasing levels of rMGU (mean rMGU values are shown in Tables 3 and 4). Because of the low myocardial uptake of tracer that occurred with intralipid infusion, myocardium could not be differentiated from blood at rest with intralipids (IL/R). Because myocardial tracer uptake increases with HIC, myocardium could readily be differentiated from blood during

TABLE 3
Plasma Substrate Levels, Insulin Levels, and Myocardial Glucose Use During 1-^{11}C-Glucose PET Study

Intervention	Arterial concentration				MGU (nmol/g/min)
	Glucose (μmol/mL)	Free fatty acids (μmol/mL)	Lactate (μmol/mL)	Insulin (μU/mL)	
HIC/R (n = 9)	5.18 ± 1.23	0.09 ± 0.05	0.82 ± 0.31	99.6 ± 33.3	612 ± 225
HIC/D (n = 2)	7.10 ± 1.66	0.81 ± 0.68	1.90 ± 0.79	221.6 ± 34.0	632 ± 314
HIC/PHEN (n = 3)	5.44 ± 0.48	0.11 ± 0.05	0.93 ± 0.46	97.7 ± 29.2	1,735 ± 1,115
IL/R (n = 3)	6.52 ± 0.49	4.60 ± 2.28	1.36 ± 0.92	12.2 ± 14.2	0 ± 0
IL/HIC (n = 2)	5.08 ± 1.15	2.84 ± 0.48	0.79 ± 0.40	77.7 ± 2.38	89 ± 4
IL/HIC/D (n = 2)	5.55 ± 0.48	3.92 ± 0.19	0.92 ± 0.41	111.7 ± 13.7	244 ± 56

MGU = myocardial glucose use measured by Fick method from glucose plasma levels; D = dobutamine.
Values represent mean ± SD.

TABLE 4
Plasma Substrate Levels, Insulin Levels, and Myocardial Glucose Use During ^{18}F-FDG PET Study

Intervention	Arterial concentration				MGU
	Glucose (μmol/mL)	Free fatty acids (μmol/mL)	Lactate (μmol/mL)	Insulin (μU/mL)	(nmol/g/min)
HIC/R (n = 9)	5.09 ± 1.51	0.07 ± 0.05	0.76 ± 0.31	114.3 ± 28.6	564 ± 240
HIC/D (n = 2)	7.21 ± 0.88	0.69 ± 0.27	1.90 ± 0.79	211.1 ± 0.35	345 ± 35
HIC/PHEN (n = 3)	5.22 ± 0.13	0.11 ± 0.06	0.98 ± 0.34	83.6 ± 22.2	1,935 ± 802
IL/R (n = 3)	7.54 ± 0.84	4.91 ± 1.67	1.36 ± 0.92	14.8 ± 11.2	60 ± 70
IL/HIC (n = 2)	4.98 ± 0.77	2.86 ± 0.58	0.80 ± 0.40	84.5 ± 19.5	35 ± 4
IL/HIC/D (n = 2)	5.35 ± 0.52	3.93 ± 0.05	0.92 ± 0.41	112.0 ± 23.2	289 ± 288

MGU = myocardial glucose use measured by Fick method from glucose plasma levels; D = dobutamine.
Values represent mean ± SD.

the clamp at rest (HIC/R) and even more so during phenylephrine (HIC/PHEN).

The ability of PET to measure myocardial uptake of the 2 tracers is shown in Figure 2. PET-derived measurements of myocardial K for either 1-^{11}C-glucose (Fig. 2A, y-axis) or ^{18}F-FDG (Fig. 2B, y-axis) correlated closely with directly measured values of tracer uptake (Fig. 2A, x-axis: 1-^{11}C-glucose K; Fig. 2B, x-axis: ^{18}F-FDG K). There were no significant differences between the regression coefficients of 1-^{11}C-glucose and ^{18}F-FDG (0.79 vs. 0.77, P = not statistically significant [NS]), and neither slope, 0.98 or 0.74, was significantly different from unity.

Shown in Figure 3 are the correlations of K values for 1-^{11}C-glucose and ^{18}F-FDG with unlabeled glucose, all measured by arterial and coronary sinus sampling. The K values for 1-^{11}C-glucose agreed closely with the K values for unlabeled glucose (Fig. 3A). The K values for ^{18}F-FDG, either uncorrected (Fig. 3B) or corrected for differences in transport and phosphorylation between ^{18}F-FDG and glucose using an LC value of 0.67 (Fig. 3C), also correlated with the K values for unlabeled glucose; however, the correlation was significantly less than that observed with 1-^{11}C-glucose ($P < 0.001$ for the comparison of correlation coefficients of 0.96 and 0.72). Moreover, K values for ^{18}F-FDG corrected using a variable LC calculated from Equation 3 (LCv) (Fig. 3D) did not significantly improve the correlation with K values for unlabeled glucose (r = 0.61, $P < 0.05$). Of note, neither 1-^{11}C-glucose nor ^{18}F-FDG (corrected by LC) underestimated the myocardial uptake of glucose (P = NS for slope values for both tracers, compared with unity). However, using the LCv underestimated the myocardial uptake of unlabeled glucose ($P < 0.001$ for a slope of 0.24, compared with unity [Fig. 4D]).

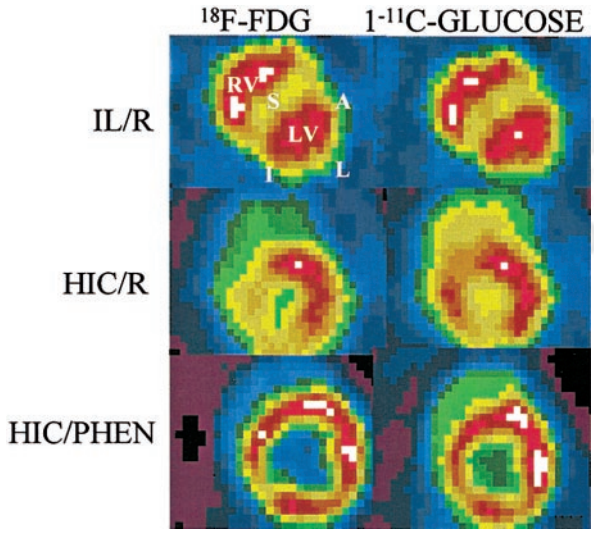

FIGURE 1. Myocardial ^{18}F-FDG and 1-^{11}C-glucose short-axis images obtained 30–60 min after injection of tracer in dogs studied during either IL/R, HIC/R, or HIC/PHEN. Black is lowest activity and white is highest activity. A = anterior; I = inferior; L = lateral; LV = left ventricle; RV = right ventricle; S = septum.

Figure 4 shows the correlation between PET-derived values for rMGU using 1-^{11}C-glucose (Fig. 4A) or ^{18}F-FDG (Figs. 4B–4D) with values for rMGU measured directly from plasma glucose levels using the Fick method over a wide range of substrate and insulin availability and levels of cardiac work. PET-derived values for rMGU obtained with 1-^{11}C-glucose correlated closely with directly measured values of rMGU (Fig. 4A). PET-derived values for rMGU obtained with ^{18}F-FDG before and after correction of data by LC values also correlated with direct measurements of rMGU (Figs. 4B–4D). Of note, using the LCv correction did not improve the correlation (Fig. 4D). Moreover, the correlation was significantly closer when 1-^{11}C-glucose, as opposed to ^{18}F-FDG, was used, regardless of whether an LC was used or the type of LC used (Figs. 4B–4D) ($P < 0.001$ for comparison of correlation coefficients). Measurements of rMGU with 1-^{11}C-glucose were underestimated by ~18% (Fig. 4A, $P < 0.001$ compared with unity). Similarly, PET with ^{18}F-FDG also underestimated rMGU by ~19%–75% depending on the whether an LC correction was used and the type of LC used (Figs. 4B–4D, $P <$ 0.001 compared with unity).

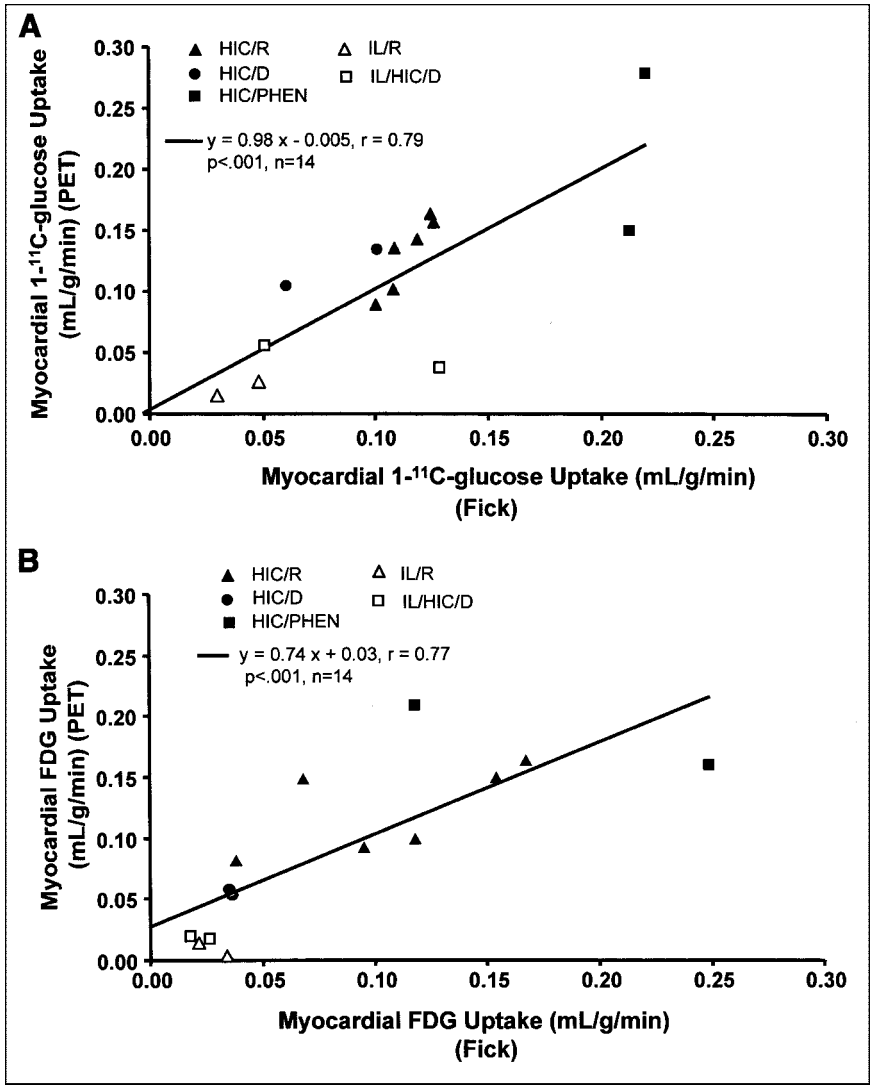

FIGURE 2. (A) Correlation between PET-derived measurements of myocardial uptake of 1-^{11}C-glucose and direct measurements of myocardial uptake of 1-^{11}C-glucose. (B) Correlation between PET-derived measurements of myocardial uptake of ^{18}F-FDG and direct measurements of myocardial uptake of ^{18}F-FDG. D = dobutamine.

Table 5 summarizes the correlation between PET-derived uptake values for 1-^{11}C-glucose and ^{18}F-FDG (dependent variables) and directly measured glucose uptake values (independent variable). Correlation coefficients for ^{18}F-FDG uptake values derived from either the Patlak method or kinetic modeling assuming no ^{18}F-FDG egress or assuming ^{18}F-FDG egress were all significantly worse than those obtained for 1-^{11}C-glucose K values (r = 0.78, 0.82, and 0.81, respectively, for ^{18}F-FDG PET vs. r = 0.97 for glucose PET, $P < 0.001$). However, there were no significant differences among the correlation coefficients for the different ^{18}F-FDG uptake values (r = 0.78, 0.82, and 0.81, respectively; P = NS).

To assess the regional variability of the PET measurements using either tracer, mean K and rMGU values were obtained from 3–5 regions of interest per study. Regional variation of PET-derived myocardial K values for 1-^{11}C-glucose and ^{18}F-FDG were similar, with COV% values of 8.0% ± 5.7% and 9.4% ± 8.11%, respectively (P = NS).

DISCUSSION

This study provided new findings on the quantification of rMGU by PET. Over a wide range of plasma substrate and insulin availability and of levels of cardiac work, myocardial uptake of 1-^{11}C-glucose more closely paralleled uptake of unlabeled glucose than did uptake of ^{18}F-FDG. As a consequence, PET measurements of rMGU were more accurate when the tracer was 1-^{11}C-glucose, as opposed to ^{18}F-FDG.

As expected, noninvasive PET measurements of myocardial uptake for both 1-^{11}C-glucose and ^{18}F-FDG correlated well with direct measurements of tracer uptake (Figs. 2A and 2B). Moreover, the observation that the myocardial uptake kinetics of 1-^{11}C-gluose more closely paralleled glucose uptake when compared with the myocardial kinetics of ^{18}F-FDG was not surprising. D-glucose labeled in the 1-carbon position with ^{11}C should have the same transport and biochemical characteristics as unlabeled D-glucose. Because uptake of D-glucose far surpasses uptake of L-glucose in

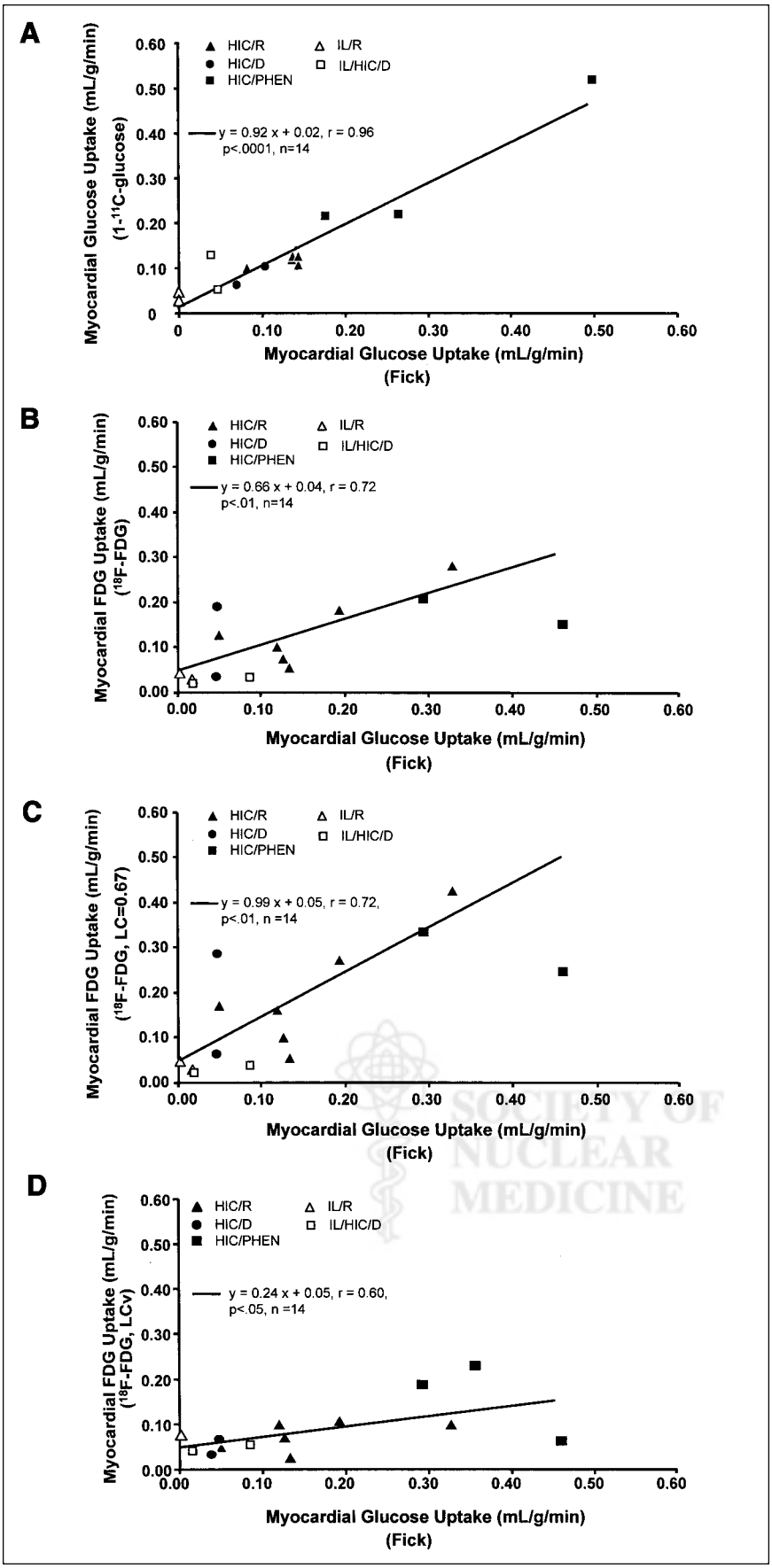

FIGURE 3. (A) Correlation between direct measurements of myocardial uptake of 1-^{11}C-glucose and unlabeled glucose. (B–D) Correlation between direct measurements of myocardial uptake of ^{18}F-FDG and unlabeled glucose for uncorrected ^{18}F-FDG K values (B), values corrected by LC (C), and values corrected by LCv (D). D = dobutamine.

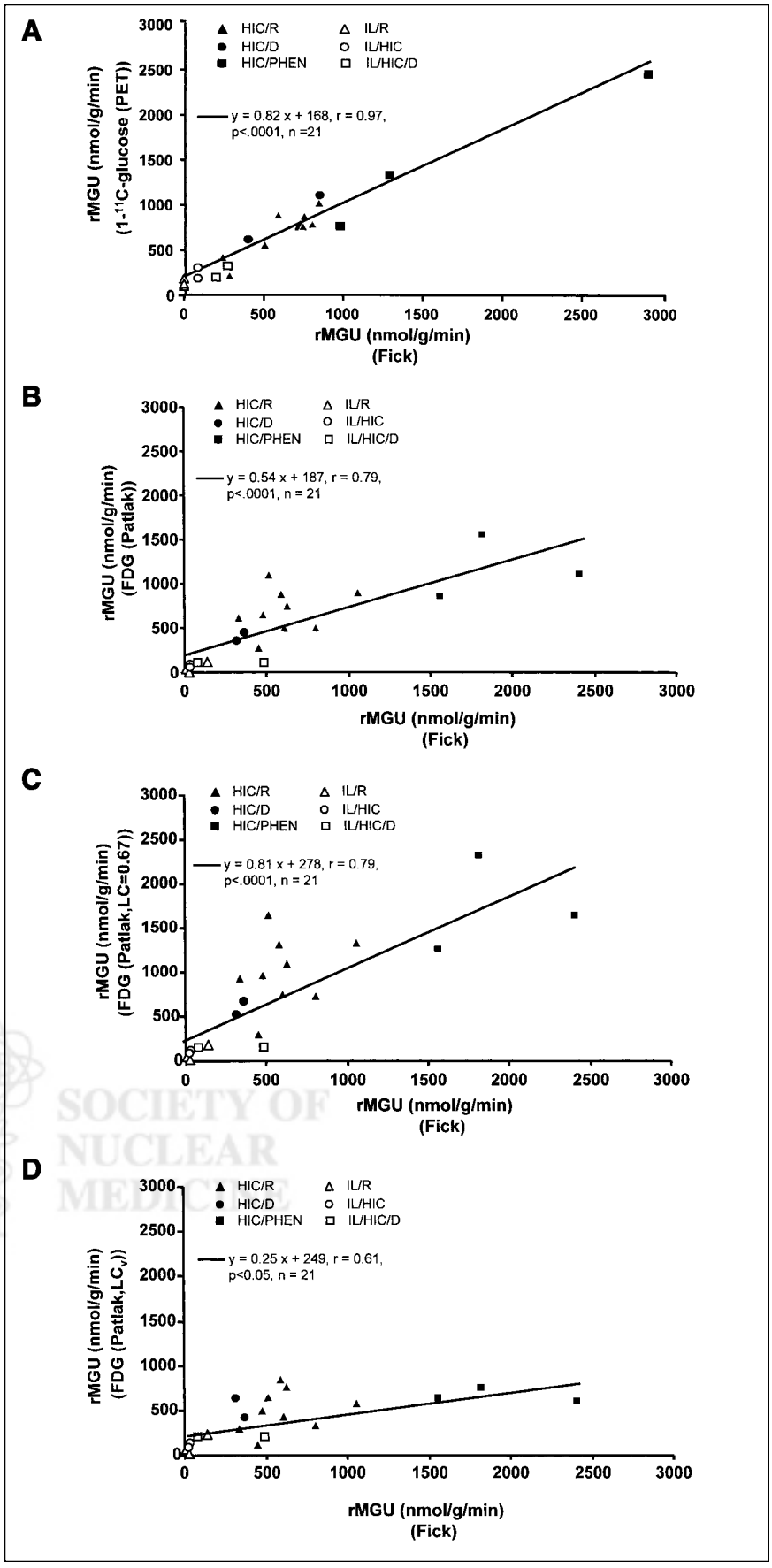

FIGURE 4. Correlation between PET-derived (*y*-axis) and Fick-derived (*x*-axis) measurements of rMGU from 1-^{11}C-glucose (A), from ^{18}F-FDG before correcting PET values (B), from ^{18}F-FDG after correcting PET values by LC (C), and from ^{18}F-FDG after correcting PET values by LCv (D). D = dobutamine.

TABLE 5
Linear Regression Analysis of PET-Derived K Values and Directly Measured Glucose K Values

Independent variable	Dependent variable	Slope	Intercept (mL/g/min)	*r*	*P* of *r*
$K_{GLUCOSE}$	$K_{PET\text{-}GLUCOSE}$	0.77 ± 0.05	0.03 ± 0.01	0.97	<0.0001
$K_{GLUCOSE}$	$K_{PET\text{-}^{18}F\text{-}FDG\text{-}PATLAK}$	0.50 ± 0.09*	0.04 ± 0.02	0.78†	<0.0001
$K_{GLUCOSE}$	$K_{PET\text{-}^{18}F\text{-}FDG\text{-}NE}$	0.75 ± 0.12	0.08 ± 0.02	0.82†	<0.0001
$K_{GLUCOSE}$	$K_{PET\text{-}^{18}F\text{-}FDG\text{-}E}$	0.52 ± 0.09*	0.004 ± 0.015	0.81†	<0.0001

*$P < 0.05$ vs. $K_{PET\text{-}GLUCOSE}$ slope.

†$P < 0.05$ vs. $K_{PET\text{-}GLUCOSE}$ correlation coefficient (*r*).

$K_{GLUCOSE}$ = glucose uptake measured directly from plasma glucose levels by Fick method; $K_{PET\text{-}GLUCOSE}$ = glucose uptake measured by PET and kinetic modeling of 1-^{11}C-glucose; $K_{PET\text{-}^{18}F\text{-}FDG\text{-}PATLAK}$ = ^{18}F-FDG uptake measured by PET and Patlak method; $K_{PET\text{-}^{18}F\text{-}FDG\text{-}NE}$ = ^{18}F-FDG uptake measured by PET and kinetic modeling of ^{18}F-FDG after assuming that ^{18}F-FDG egress is negligible; $K_{PET\text{-}^{18}F\text{-}FDG\text{-}E}$ = ^{18}F-FDG uptake measured by PET and kinetic modeling of ^{18}F-FDG after assuming that ^{18}F-FDG egress is not negligible.

Data in Slope and Intercept columns represent estimated values from linear regression analysis and their corresponding SEs.

muscle, uptake of 1-^{11}C-glucose should be nearly identical to that of unlabeled glucose (*30*). Indeed, the close and direct correlation between direct measurements of 1-^{11}C-glucose and unlabeled glucose uptake supports this assumption (Fig. 3A). In contrast, ^{18}F-FDG is an analog of glucose whose kinetics parallel only the transmembranous transport and hexokinase-mediated phosphorylation of glucose. To account for the differences between ^{18}F-FDG and glucose, the LC was devised so that PET measurements of rMGU could be performed (*6–10*). However, values for the LC have been shown to depend markedly on the availability of various plasma substrates such as lactate and fatty acids, the level of insulin, and the level of blood flow (*11–15*). Variability in the LC likely contributed to the poorer correlation of direct measurements of myocardial ^{18}F-FDG uptake with those of unlabeled glucose.

A solution has been proposed to calculate the LC on the basis of the application of assumptions underlying Michaelis–Menten kinetics to the conventional 3-compartment model describing myocardial ^{18}F-FDG kinetics (*16*,*26*). Although initial results obtained in isolated perfused hearts are promising, the approach assumes that the ratios of ^{18}F-FDG to glucose for transport and initial phosphorylation are constant—an assumption that is unproven. Moreover, the approach does not account for LC variability due to changes in MBF (*15*). In the present study, variable LC values calculated from Equation 3 ranged from 0.49 ± 0.04 in the intralipid intervention at rest, which had the highest levels of plasma fatty acids, to 1.75 ± 0.36 in the clamp/phenylephrine group. Furthermore, results from multiple linear regression analysis showed a significant correlation between LCv values with MBF and plasma glucose, free fatty acid, lactate, and insulin levels ($r = 0.84$, $P < 0.001$), with free fatty acids and insulin being significant negative predictors of LCv values ($P < 0.0001$ and $P < 0.05$, respectively). Thus, in the present study, the pattern of LCv changes with changing plasma levels of insulin and fatty acids is consistent with what is known about the impact of these variables on the relationship between ^{18}F-FDG and glucose transport and phosphorylation (*11–14*). The poor correlation between myocardial uptake of ^{18}F-FDG and unlabeled glucose when LCv was used (Fig. 3D) suggests that this approach may be of limited value in vivo, a setting in which the integrative effects of plasma insulin and fatty acid levels and MBF are operational.

Although the myocardial kinetics of 1-^{11}C-glucose more faithfully trace those of glucose than do the myocardial kinetics of ^{18}F-FDG, this advantage would be minimized if the myocardial kinetics of 1-^{11}C-glucose could not be quantified accurately with PET. Clearly, compartmental modeling is more demanding with 1-^{11}C-glucose than it is with ^{18}F-FDG. The arterial input function must be corrected for the production of $^{11}CO_2$ as well as ^{11}C-lactate. Moreover, the complexity is also exacerbated by the more diverse metabolic fates of 1-^{11}C-glucose, compared with the metabolic fates of ^{18}F-FDG. Finally, because of significant egress of tracer from the myocardium, more simplified approaches to quantify tracer uptake, such as Patlak graphical analysis, as is done with ^{18}F-FDG, cannot be used with 1-^{11}C-glucose. Despite the more complex kinetics of 1-^{11}C-glucose compared with those of ^{18}F-FDG, PET quantification of myocardial glucose uptake was more accurate with 1-^{11}C-glucose than with ^{18}F-FDG (Fig. 3). As a consequence, PET measurements of rMGU were more accurate when 1-^{11}C-glucose, as opposed to ^{18}F-FDG, was used as the tracer, regardless of whether an LC correction was implemented or the type of correction used (Fig. 4).

There was slight, ~18%, underestimation of rMGU by PET with 1-^{11}C-glucose (Fig. 4A). Given that direct measurements of 1-^{11}C-glucose uptake did not underestimate unlabeled glucose uptake (Fig. 3A) and that PET did not underestimate 1-^{11}C-glucose uptake (Fig. 2A), it is unlikely that the underestimation of rMGU either was due to tracer effects or was the result of compartmental modeling. Indeed, the underestimation of rMGU appears to be mainly due to underestimation of the highest glucose use value, 3,000 nmol/g/min. Removal of this value resulted in a similar regression value of 0.95 (vs. 0.97), with a slope of

0.92 (P = NS from a slope value of 1). Values of rMGU obtained from uncorrected Patlak K values were significantly underestimated (Fig. 4B). Correction of the K values by a constant LC value of 0.67 resulted in a regression slope not different from 1 (Fig. 4C). In contrast, correction of K values by LCv worsened the underestimation of rMGU (Fig. 4D). As already mentioned, this result was most probably due to the limited value of the LCv approach in a complex environment in which substrate and insulin plasma levels, as well as myocardial perfusion, play key roles in the competitive myocardial kinetics of ^{18}F-FDG and glucose. In fact, further investigation of the LCv values obtained in our study showed that those obtained from the interventions that resulted in high glucose uptake values (greater than 0.15 mL/g/min) were the key contributors to the underestimation of rMGU. Exclusion of these studies from the regression analysis (all 3 clamp/phenylephrine studies and 3 clamp/rest studies) resulted in improved correlation and slope between rMGU measured with ^{18}F-FDG and direct measurements of rMGU ($y = 0.94x + 71$, $r = 0.82$, $P < 0.0001$, $n = 15$). Thus, correction of ^{18}F-FDG kinetics using tracer kinetic information as described by Botker et al. (*16*) appears to break down for high values of glucose uptake.

The results of previous studies on animals and humans have shown a closer correlation between ^{18}F-FDG and glucose, regardless of whether myocardial uptake or rMGU was measured, than we observed in the current study (Figs. 3 and 4). This worse correlation in our study was not due to the method of analysis chosen. The correlation between myocardial ^{18}F-FDG uptake and unlabeled glucose uptake was similar regardless of whether compartmental modeling or the Patlak method was used to analyze myocardial ^{18}F-FDG kinetics (Table 5). However, in the earlier studies, the level of MBF was not varied and fatty acid levels were either raised (by fasting) or reduced (by adding insulin). In contrast, in the current study, we measured myocardial ^{18}F-FDG kinetics while varying all 3 of these parameters simultaneously.

We studied the accuracy of rMGU using these 2 tracers over a wide range of substrate availability, insulin levels, and cardiac work. As mentioned previously, these interventions were chosen because studies have shown that these factors may alter the LC significantly (*11–15*). Furthermore, these interventions have physiologic and clinical relevance. Marked elevations in levels of plasma fatty acids either alone or together with hyperinsulinemia are observed during intense exercise or in non–insulin-dependent diabetes mellitus, respectively (*31*,*32*). Moreover, under conditions of stress, one could also see an increase in MBF, further increases in plasma catecholamines, and then increases in plasma fatty acids due to the lipolytic effects of these hormones (*33*). Although the superiority of 1-^{11}C-glucose over ^{18}F-FDG for quantifying rMGU for PET has been shown under these conditions, it is unknown whether similar advantages will be observed under pathologic conditions such as left ventricular hypertrophy, diabetic heart disease, and myocardial ischemia and reperfusion.

CONCLUSION

This study has demonstrated that PET measurements of rMGU are more accurate when 1-^{11}C-glucose is used instead of ^{18}F-FDG. The improved accuracy most likely reflects the more faithful tracing of myocardial glucose uptake with 1-^{11}C-glucose than with ^{18}F-FDG. However, the results of the current study do not negate the wealth of information about the usefulness of PET and ^{18}F-FDG to measure either relative or absolute rMGU in heart disease. For example, the key role of relative estimates of rMGU measured by PET and ^{18}F-FDG in differentiating viable from nonviable myocardium are well established. Moreover, quantitative measurements of rMGU by PET and ^{18}F-FDG have furthered our understanding of the role of alterations in myocardial metabolism in a variety of disease processes, such as myocardial ischemia and reperfusion, dilated cardiomyopathy, and diabetic heart disease. However, the results of the current study do suggest that in situations in which absolute rates of rMGU are required, PET imaging with 1-^{11}C-glucose may provide an advantage over PET imaging with ^{18}F-FDG.

ACKNOWLEDGMENTS

We thank Mary Russo for her administrative assistance. This study was supported by grant HL13581 from the National Institutes of Health.

REFERENCES

1. Czernin J, Porenta G, Brunken R, et al. Regional blood flow, oxidative metabolism, and glucose utilization in patients with recent myocardial infarction. *Circulation.* 1993;88:884–895.
2. Nienaber CA, Gambhir SS, Mody FV, et al. Regional myocardial blood flow and glucose utilization in symptomatic patients with hypertrophic cardiomyopathy. *Circulation.* 1993;87:1580–1590.
3. Maki M, Luotolahti M, Nuutila P, et al. Glucose uptake in the chronically dysfunctional but viable myocardium. *Circulation.* 1996;93:1658–1666.
4. Wallhaus TR, Taylor M, DeGrado TR, et al. Myocardial free fatty acid and glucose use after carvedilol treatment in patients with congestive heart failure. *Circulation.* 2001;103:2441–2446.
5. Herrero P, Weinheimer CJ, Dence C, et al. Quantification of myocardial glucose utilization by positron emission tomography and 1-^{11}C-glucose. *J Nucl Cardiol.* 2002;9:5–14.
6. Ratib O, Phelps ME, Huang S-C, et al. Positron tomography with deoxyglucose for estimating local myocardial glucose metabolism. *J Nucl Med.* 1982;23:577–586.
7. Krivokapich J, Huang S-C, Phelps ME, et al. Estimation of rabbit myocardial metabolic rate for glucose using fluorodeoxyglucose. *Am J Physiol.* 1982;243:H884–H895.
8. Gambhir SS, Schwaiger M, Huang S-C, et al. Simple noninvasive quantification method for measuring myocardial glucose utilization in humans employing positron emission tomography and fluorine-18 deoxyglucose. *J Nucl Med.* 1980;30:359–366.
9. Choi Y, Hawkins RA, Huang S-C, et al. Parametric images of myocardial metabolic rate of glucose generated from dynamic cardiac PET and 2-[^{18}F]fluoro-2-deoxy-d-glucose studies. *J Nucl Med.* 1991;32:733–738.
10. Depre C, Vanoverschelde JL, Taegtmeyer H. Glucose for the heart. *Circulation.* 1999;99:578–588.
11. Hariharan R, Bray M, Ganim R, et al. Fundamental limitations of [^{18}F]2-deoxy-2-fluoro-D-glucose for assessing myocardial glucose uptake. *Circulation.* 1995;91:2435–2444.

12. Marshall RC, Powers-Risius P, Huesman RH, et al. Estimating glucose metabolism using glucose analogs and two tracer kinetic models in isolated rabbits. *Am J Physiol.* 1998;44:H668–H679.
13. Botker HE, Bottcher M, Schmitz O, et al. Glucose and lumped constant variability in normal human hearts determined with ^{18}F-fluorodeoxyglucose. *J Nucl Cardiol.* 1997;4:125–132.
14. Hashimoto K, Nishimura T, Imahashi KI, et al. Lump constant for deoxyglucose is decreased when myocardial glucose uptake is enhanced. *Am J Physiol.* 1999; 45:H129–H133.
15. McFalls EO, Baldwin D, Marx D, at al. Effect of regional hyperemia on myocardial uptake of 2-deoxy-2-[^{18}F]fluoro-D-glucose. *Am J Physiol Endocrinol Metab.* 2000;278:E96–E102.
16. Botker HE, Goodwin GW, Holden JE, at al. Myocardial glucose uptake measured with fluorodeoxyglucose: a proposed method to account for variable lump constants. *J Nucl Med.* 1999;40:1186–1196.
17. Powers WJ, Dagago-Jack S, Markham J, et al. Cerebral transport and metabolism of 1-^{11}C-D-glucose during stepped hypoglycemia. *Ann Neurol.* 1995;38:599–608.
18. Powers WJ, Rosenboum JL, Dence CS, et al. Cerebral transport and metabolism in preterm human infants. *J Cereb Blood Flow Metab.* 1998:18:632–638.
19. Stone-Elander S, Halldin C, Langstrom B, et al. Method for routine production of 1-^{11}C-D-glucose from ^{11}C-ammonium cyanide. *J Nucl Med.* 1989;5:927–931.
20. Dence CS, Powers WJ, Welch MJ. Improved synthesis of 1-^{11}C-D-glucose. *Appl Radiat Isot.* 1993;44:971–980.
21. Bergmann SR, Herrero P, Markham J, et al. Noninvasive quantitation of myocardial blood flow in human subjects with oxygen-15-labeled water and positron emission tomography. *J Am Coll Cardiol.* 1989;14:639–652.
22. Herrero P, Markham J, Bergmann SR. Quantitation of myocardial blood flow with $H_2{}^{15}O$ and positron emission tomography: assessment and error analysis of a mathematical approach. *J Comput Assist Tomogr.* 1989;13:862–873.
23. Herrero P, Hartmann JJ, Senneff MJ, et al. Effects of time discrepancies between input and myocardial time-activity curves on estimates of regional myocardial perfusion with PET. *J Nucl Med.* 1994;35:558–566.
24. Gear CW. Numerical initial-value problems in ordinary differential equations. Englewood Cliffs, NJ: Prentice-Hall; 1971.
25. Dennis, JE, Schnabel RB. Numerical methods for unconstrained optimization and nonlinear equations. Englewood Cliffs, NJ: Prentice-Hall; 1983.
26. Wiggers H, Botcher M, Nielsen TT, et al. Measurement of myocardial glucose uptake in patients with ischemic cardiomyopathy: application of a new quantitative method using regional tracer information. *J Nucl Med.* 1999;40:1292–1300.
27. Morgan CR, Lavora A. Immunoassay of insulin: two antibody system. *Diabetes.* 1963;12:115–120.
28. Haastrup AT, Stepniakowski KT, Goodfriend TL, et al. Intralipid enhances alpha-1 receptor-mediated pressor sensitivity. *Hypertension.* 1998;32:693–698.
29. Steinberg HO, Tarshoby M, Monestel R, et al. Elevated circulating free fatty acid levels impair endothelium-dependent vasodilation. *J Clin Invest.* 1997; 100:1230–1239.
30. Maclean DA, Ettinger SM, Sinoway LI, et al. Determination of muscle-specific glucose flux using radioactive stereoisomers and microdialysis. *Am J Physiol Endocrinol Metab.* 2001;280:E187–E192.
31. Skowronski R, Hollenbeck CB, Varasteh BB, et al. Regulation of non-esterified fatty acid and glycerol concentration by insulin in normal individuals and patients with type 2 diabetes. *Diabet Med.* 1991;8:330–333.
32. Bülow J. Lipid mobilization and utilization. In: Poortmans JR, ed. *Principles of Exercise Biochemistry.* 2nd ed. Basel, Switzerland: Karger; 1993:158–185.
33. Large V, Arner P. Regulation of lipolysis in humans: pathophysiological modulation in obesity, diabetes, and hyperlipidaemia. *Diabetes Metab.* 1998;24:409–418.

JNM The Journal of NUCLEAR MEDICINE

Comparison of 1-^{11}C-Glucose and ^{18}F-FDG for Quantifying Myocardial Glucose Use with PET

Pilar Herrero, Terry L. Sharp, Carmen Dence, Brendan M. Haraden and Robert J. Gropler

J Nucl Med. 2002;43:1530-1541.

The Journal of Nuclear Medicine is published monthly.
SNMMI | Society of Nuclear Medicine and Molecular Imaging
1850 Samuel Morse Drive, Reston, VA 20190.
(Print ISSN: 0161-5505, Online ISSN: 2159-662X)

SNMMI SOCIETY OF NUCLEAR MEDICINE AND MOLECULAR IMAGING